OXFORD

ORIGINAL ARTICLE

Small Nucleus Accumbens and Large Cerebral Ventricles in Infants and Toddlers Prior to Receiving Diagnoses of Autism Spectrum Disorder

Tadashi Shiohama [1,a], Alpen Ortug[1,b,c], Jose Luis Alatorre Warren [1,b,c], Briana Valli[1,d], Jacob Levman[2], Susan K. Faja[3], Keita Tsujimura[4,5], Alika K. Maunakea[6] and Emi Takahashi[1,b,c]

[1]Division of Newborn Medicine, Department of Medicine, Boston Children's Hospital, Harvard Medical School, Boston, MA 02115, USA, [2]Department of Mathematics, Statistics and Computer Science, St. Francis Xavier University, Antigonish, Nova Scotia B2G 2W5, Canada, [3]Division of Developmental Medicine, Department of Medicine, Boston Children's Hospital, Harvard Medical School, Boston, MA 02115, USA, [4]Group of Brain Function and Development, Nagoya University Neuroscience Institute of the Graduate School of Science, Furo-cho, Chikusa-ku, Nagoya, Aichi 464-8602, Japan, [5]Research Unit for Developmental Disorders, Institute for Advanced Research, Nagoya University, Furo-cho, Chikusa-ku, Nagoya, Aichi 464-8602, Japan and [6]Department of Anatomy, Biochemistry and Physiology, 651 Ilalo Street, John A. Burns School of Medicine, University of Hawaii, Manoa, HI 96813, USA

Current addresses for authors [a]Department of Pediatrics, Chiba University Hospital, Chiba 2608670, Japan, [b]Athinoula A. Martinos Center for Biomedical Imaging, Massachusetts General Hospital, Charlestown, Massachusetts, USA, [c]Department of Radiology, Harvard Medical School, Boston, Massachusetts, USA, [d]Behavioral Neuroscience Program, Northeastern University, Boston, MA 02115, USA.
Address correspondence to Tadashi Shiohama, M.D., Ph.D., Boston Children's Hospital, 300 Longwood Avenue, Boston, MA 02115, USA.
Email: asuha_hare@yahoo.co.jp

Abstract

Early interventions for autism spectrum disorder (ASD) are increasingly available, while only 42–50% of ASD children are diagnosed before 3 years old (YO). To identify neuroimaging biomarkers for early ASD diagnosis, we evaluated surface- and voxel-based brain morphometry in participants under 3YO who were later diagnosed with ASD. Magnetic resonance imaging data were retrospectively obtained from patients later diagnosed with ASD at Boston Children's Hospital. The ASD participants with comorbidities such as congenital disorder, epilepsy, and global developmental delay/intellectual disability were excluded from statistical analyses. Eighty-five structural brain magnetic resonance imaging images were collected from 81 participants under 3YO and compared with 45 images from 45 gender- and age-matched nonautistic controls (non-ASD). Using an Infant FreeSurfer pipeline, 236 regionally distributed measurements were extracted from each scan. By *t*-tests and linear mixed models, the smaller nucleus accumbens and larger bilateral lateral, third, and fourth ventricles were identified in the ASD group. Vertex-wise *t*-statistical maps showed decreased thickness in the caudal anterior cingulate cortex and increased thickness in the right medial orbitofrontal cortex in ASD. The smaller bilateral accumbens nuclei and larger cerebral ventricles were independent of age, gender, or gestational age at birth, suggesting that there are MRI-based biomarkers in prospective ASD patients before they receive the diagnosis and that the volume of the nucleus accumbens and cerebral ventricles can be key MRI-based early biomarkers to predict the emergence of ASD.

Introduction

Autism spectrum disorder (ASD) is a complex neurodevelopmental disorder characterized by deficits in social communication and interaction and restricted and repetitive patterns of behaviors, interests, and activities (The American Psychiatric Association 2013; Maenner et al. 2014; Kim et al. 2014). ASD prevalence is estimated as 1 in 59 children aged 8 years in 2014 in the USA (Baio et al. 2018). Early therapeutic interventions for children with ASD are increasingly available, including intensive behavior intervention (Dawson et al. 2010; Howard et al. 2014; Zwaigenbaum et al. 2015; Rogers et al. 2019), and biological approaches such as molecular targeting (Green and Garg 2018) and genetic therapies (Benger et al. 2018). Despite the development of early interventions for ASD, only 42–50% of ASD children were diagnosed before 3 years old (Soke et al. 2017; Baio et al. 2018). Additionally, early intervention is generally considered to be advantageous because it potentially enables intervention to be delivered during a sensitive period of development and when children have not yet fallen as far behind their peers without ASD (Zwaigenbaum et al. 2015; Vivanti et al. 2018). Therefore, the exploration of highly effective tools for early ASD diagnosis is an important research goal.

Structural brain magnetic resonance imaging (MRI) measurements (Hazlett et al. 2005, 2011, 2012, 2017; Schumann et al. 2010; Wolff et al. 2015; Swanson et al. 2017) as well as salivary micro ribonucleic acid (Hicks et al. 2016) and resting-state electroencephalogram measures (Duffy and Als 2012; Heunis et al. 2016) have been proposed as potential biomarkers for early diagnosis of ASD. One of the major challenges of performing an ASD study is its heterogeneous clinical symptoms with various comorbid disorders in the ASD population. Because there is growing evidence that abnormal structural brain morphology precedes the emergence of cognitive delay and language problems, it is important to examine structural MRI data from early developmental ages. However, structural brain MRI scans are rarely obtained in early childhood prior to diagnosis of ASD. Therefore, prior structural brain MRI studies focused on infants with high genetic risk for ASD who were studied prospectively (Hazlett et al. 2012, 2017) but are limited because children later diagnosed with ASD are a small proportion in the enrolled population. Additionally, these studies focused on children with a particular type of familial risk for ASD who may not fully represent the population of children with ASD (i.e., some children with ASD may have different risk factors like de novo genetic events).

The goal of this study is to identify candidate neuroimaging biomarkers or subclinical indicators for early diagnosis of ASD through the surface- and voxel-based brain morphology MRI analyses. The regional surface-based approach was used to identify candidate measurements for predicting ASD, and additionally, the vertex-based approach was used to identify fine areas with changes of cortical thickness, which could not be identified by the regional approach.

Patients and Methods

Patients

Following approval by the Institutional Review Board at Boston Children's Hospital (BCH), we reviewed clinical brain MR images and electronic medical records with over 145 000 examinations from 1 January 2008 to 24 February 2016, to assemble a cohort of patients with ASD. After exclusion of examinations with technical errors such as low-quality images and image-processing failure, 1003 examinations from 781 participants were collected (Levman et al. 2017, 2018a, 2018b, 2019).

All participants were diagnosed with ASD, or pervasive developmental disorder according to DSM-IV or DSM-5 by child neurologists, developmental pediatricians, or child psychiatrists at BCH. We included participants with age at the examination under 3 years old and followed at least until the age of 4 years. The leading reasons for the MRI examination in participants with ASD are global developmental delay/intellectual deficiency (GDD/ID) (26%), hyperactivity (16%), epilepsy (13%), headache (10%), and abdominal symptoms (14%). Cases with congenital disorders or other destructive brain disorders, including perinatal brain injuries and encephalopathy, were carefully excluded, according to a flowchart of participant selection (Fig. 1). We also carefully excluded genetic disorders, including congenital disorders with ASD and/or macrocephaly such as Sotos syndrome (Srour et al. 2006), PTEN hamartoma tumor syndrome (Kato et al. 2018; Shiohama et al. 2020), tuberous sclerosis complex (Fidler et al. 2000), and CHD8 mutations (Bernier et al. 2014). We also excluded ASD participants with epilepsy and/or GDD/ID because the presence of epilepsy and GDD/ID are potential confounders for structural brain changes. Almost all of the MRI scans were carried out prior to the ASD diagnosis. Forty-five examinations from 45 gender- and age-matched nonautistic controls (non-ASD) were assembled retrospectively in previous analyses (Levman et al. 2017, 2018a, 2018b, 2019) by selecting participants based on a normal MRI examination, as assessed by a BCH neuroradiologist, and whose medical records provided no indication of any neurological problems. The leading reasons for the MRI examination in non-ASD were headaches (60%), to rule out intracranial pathologies (13%), vomiting (11%), and night awakenings (10%). Both scans (ASD and non-ASD) were acquired at BCH.

MRI Acquisition and Processing

Three-dimensional T1-weighted structural images (TR 1130–2530 ms; TE 1.69–2.52 ms, FOV = 220, matrix 192–256 × 192–256) were obtained with four clinical 3 T MRI scanners of the same model (Skyra, Siemens Medical Systems, Erlangen, Germany) from both ASD and non-ASD participants at BCH. The MR scanning was performed in ASD and non-ASD participants under natural sleep or sedation. The qualities of the acquired images were visually checked by two neuroscientists (J.L. and T.S.), and images with poor qualities were excluded from analyzes despite motion correction. Because of the clinical and retrospective nature of this study, there is variability in the pulse sequences employed to acquire T1-weighted MRI. The acquisition parameters and scanners for each image were summarized in Supplementary Material 1. Spatial resolution varied in the x- and y-directions from 0.47 to 1.1 mm (mean: 0.90 mm, standard deviation [SD]: 0.11 mm). Through-plane slice thickness varied from 0.8 to 2.0 mm (mean: 1.00 mm, SD: 0.25 mm). DICOM files were accessed through the Children's Research and Integration System (Pienaar et al. 2015) and
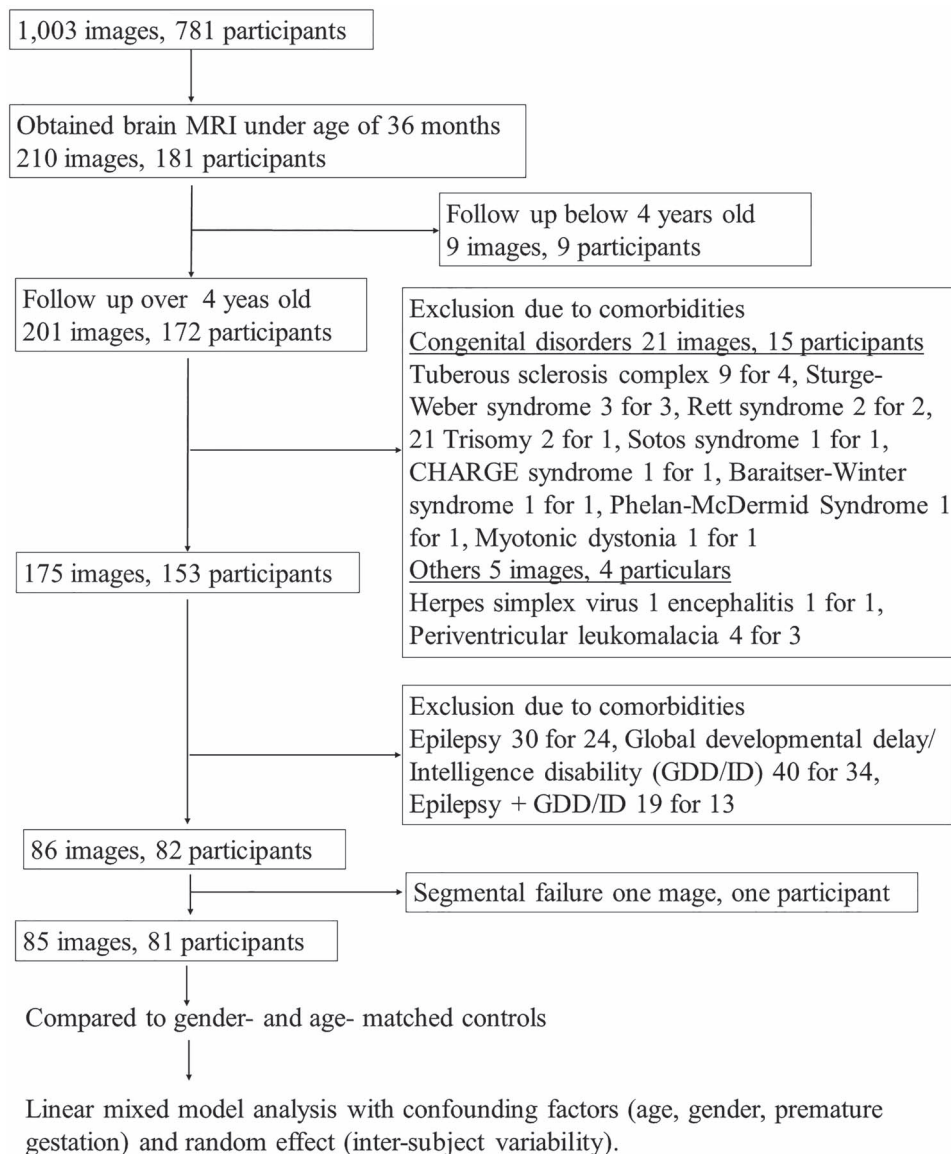
Figure 1. Flowchart of participant selection from patients with ASD.

analyzed with *recon-all* command on Infant FreeSurfer (Fischl 2012; de Macedo et al. 2015; Zöllei et al. 2020). Automatic regional segmentation by Infant FreeSurfer was visually qualified on the graphic interface of FreeView (http://surfer.nmr.mgh.harvard.edu/). There was incomplete segmentation of basal ganglia in a participant with ASD of 7 months old; thus, we excluded the patient's data from subsequent statistical analyses.

We chose not to perform manual editing for handling recon-all procedures to avoid arbitrary modifications and to ensure reproducibility. A recent review article also mentioned that changes in morphological estimates after manual interventions do not indicate a change in the quality of the data (Monereo-Sánchez et al. 2021).

Quantified measurements were extracted using brain atlases; the "brainvol" for global measurements of brain volumes, the "aseg" (Fischl et al. 2002) for segmentation of subcortical regions including the basal ganglia, cerebellum, and brainstem and the "aparc" (Desikan et al. 2006) for automatic cortical parcellation. The 26 volumes and 204 regionally distributed measurements (regional volume, surface area, and cortical thickness) were extracted from the "aseg" (Fischl et al. 2002) and the "aparc" (Desikan et al. 2006) in each subject, respectively. After excluding cases with failures of MRI processing, our study included 85 structural brain MR images from 81 ASD participants. Example segmentation results according to the "aseg" (Fischl et al. 2002) and the "aparc" (Desikan et al. 2006) annotation format for both ASD and non-ASD group are shown in Supplementary Material 2.

For group analyses of regional cortical thickness, cortical thickness maps of all individual participants were resampled onto the fsaverage template (MNI 305 space [Collins et al. 1994]) and spatially smoothed at a 10 mm full-width/half-maximum using Infant Freesurfer's *mris_preproc* and *mri_surf2surf* commands. A linear mixed model (LMM) was used to evaluate the

effect of the diagnosis of ASD on cortical thickness using Infant FreeSurfer's *mri_glmfit* command for all participants. The vertex-wise *t*-statistical map between ASD and non-ASD was visualized on the inflated surface map.

Global Developmental Delay and Intellectual Disability

GDD/ID in ASD participants was estimated by existing developmental or intellectual testing. GDD/ID was assessed with the value of (i) functional intelligence quotient of Wechsler Intelligence Scale for Children-IV or -V in 3 cases, Wechsler Preschool and Primary Scale of Intelligence-III or -IV in 5 cases, or Stanford-Binet Intelligence Scales for Early Childhood-5 in 2 cases, (ii) cognitive composite of Bayley Scales of Infant and Toddler Development-III in 26 cases, or Battelle Developmental Inventory-2 in 9 cases, (iii) general cognitive ability of Differential Ability Scales-II in 6 cases, (iv) early learning composite of Mullen Scales of Early Learning in 9 cases, or other tests in the other cases. A standard score of 70, indicating two standard deviations below the average, was determined as the cut-off point across these tests.

Statistical Analysis

The equality of means in each measurement of brain morphology between ASD and non-ASD participants was evaluated through the Levene's test for equality of variances, two-tailed unpaired *t*-tests, and the Cohen's *d* statistic. Benjamini-Hochberg critical values (Benjamini et al. 2001; Reiner et al. 2003) for controlling the false discovery rate (FDR) ($q = 0.25$) were determined as 0.042 for 6 repeating *t*-tests for global measurements, and 0.058 for 26 repeating *t*-tests for "aseg" (Fischl et al. 2002) measurements, but not determined for 204 repeating *t*-tests for "aparc" (Desikan et al. 2006) measurements. For each "aseg" (Fischl et al. 2002) and "aparc" (Desikan et al. 2006) measurements, the Linear Mixed Model (LMM) ($P < 0.05$) was used to evaluate the effects of continuous or binary covariates (age, gender, and prematurity [< 37 weeks of gestation]). The random effect was included in the model to account for intrasubject correlation. Statistical tests were computed using IBM SPSS Statistics version 19 (IBM Corp., Armonk, NY).

Results

Participants' Background

Ages at MRI scans were not different ($t(86) = 1.63$, $P = 0.106$) between ASD and non-ASD on an unpaired *t* test (the mean $\pm$ SD [range] were 24.2 ± 6.9 [9–35] and 22.1 ± 7.3 [10–35] months old in ASD [male, $n = 74$; female, $n = 11$] and non-ASD [male, $n = 38$; female, $n = 7$] participants, respectively). Among ASD participants, 25.9% (22/85) were prematurely born, while 13.3% (6/45) of the non-ASD particitants were prematurely born (Supplementary Material 3). The range of the gestation weeks at birth is 28–40 and 30–40 weeks in ASD and non-ASD participants, respectively.

Four MRI scanners ("Scanner 1," "Scanner 2," "Scanner 3," and "Scanner 4") were used in this study. The images were obtained with "Scanner 1" in 29/85 and 16/45, "Scanner 2" in 46/85 and 18/45, "Scanner 3" in 9/85 and 11/45, and "Scanner 4" in 1/85 and 0/45, in ASD and non-ASD participants, respectively. There was no statistically significant difference in the rate of the MRI scanners used for ASD and non-ASD participants (Pearson's Chi-square test, $\chi^2(3) = 5.41$, $P = 0.144$).

Voxel- and Surface-Based Brain Morphology Measurements

The estimated total intracranial volume and the volumes of the cortical and subcortical gray matter (GM) and white matter (WM) were not significantly different between ASD and non-ASD participants (Table 1), while the volumes of the cerebral ventricles and choroid plexus were larger in ASD participants than non-ASD participants ($t(128) = 2.75$, $P = 6.8 \times 10^{-3}$) (Table 1).

Surface-based vertex-wise *t*-statistical maps showed decreased cortical thickness in a part of the left caudal anterior cingulate cortex and increased cortical thickness in the right medial orbitofrontal cortex (mOF) with low *P*-values ($P < 0.0001$) (Fig. 2).

Among the 230 measurements generated from the "aseg" (Fischl et al. 2002) and "aparc" (Desikan et al. 2006) pipelines, the volumes of the left and right nucleus accumbens (NAc) in the "aseg" (Fischl et al. 2002) annotation atlas were statistically significantly smaller in ASD than non-ASD participants, and the volumes of the cerebral fluid spaces consisted of bilateral lateral ventricles, and third and fourth ventricles were larger in ASD than non-ASD participants (Table 2 and Supplementary Material 4). The other measurements, including the volumes of subcortical structures and the cortical measurements, did not significantly differ in unpaired *t*-tests (Supplementary Materials 4 and 5). There were no significant differences among measurements of cortical surface area and cortical thickness in the *t*-test (Supplementary Material 5) and among measurements of cortical surface area in the LMM (Supplementary Material 6). No significant differences were additionally identified among measurements in the *t*-test, even when selecting $q = 0.5$ for the FDR.

The effect of covariates on the 230 brain morphologic measurements was evaluated with the LMM (Table 3 and Supplementary Material 6). The diagnosis of ASD was the significant independent factor in the volumes of the bilateral NAc, cerebral ventricles (bilateral lateral ventricles, third ventricle, fourth ventricle), and the left pallidum, and the thickness in the left caudal anterior cingulate. The volume of the left pallidum and the thickness in the left caudal anterior cingulate were also dependent on the variety of MRI scanners (Table 3).

The total volume of the cortical GM, WM and subcortical GM, and the total cortical surface area demonstrated no disparity between participants with ASD and non-ASD (upper panels of Fig. 3), while cerebral ventricles and choroid plexus volume and the NAc volume demonstrated a disparity starting from the infantile period (lower panels of Fig. 3).

The average thickness of the right mOF had a negative association to the right NAc volume in the ASD group, but that was confirmed by analysis between the mOF cortical volume and the right NAc volume (Supplementary Material 7, left and middle panels). Additionally, the right amygdala volume had a positive association to the right accumbens area volume (Supplementary Material 7, right panel).

Receiver operating characteristic (ROC) curves for predicting the later diagnosis of ASD showed that the area under the curve (AUC) were 0.628, 0.655, and 0.683, for the values of the NAc volume, cerebral ventricles volume, and the rate of the NAc volume to the cerebral ventricles volume in the "aseg" annotation, respectively (Fig. 4). The cut-off values with the largest Youden index were 870 mm³ (sensitivity 0.62, specificity 0.62), 9198 mm³ (sensitivity 0.93, specificity 0.33), and 0.073 (sensitivity 0.67, specificity 0.60) for the values of the NAc volume, cerebral

Table 1 Global measurements of brain volume in Infant FreeSurfer recon-all measurements in ASD and non-ASD participants

Measurements of global anatomical classification ("brainvol")	ASD (85 images) Mean [SD]	Non-ASD (45 images) Mean [SD]	t	df	P-value	Absolute Cohen's d
eTIV	1 113 307 [118 903]	1 079 535 [104 288]	1.61	128	0.11	0.30
Total cortical GM volume (mm³)	525 983 [70 737]	516 441 [66 238]	0.75	128	0.46	0.14
Total cortical surface area (mm²)	116 631 [19 555]	113 017 [19 667]	1.00	89.3	0.32	0.18
Total cortical WM volume (mm³)	295 192 [55 054]	278 167 [49 003]	1.74	128	0.084	0.32
Total subcortical GM volume (mm³)	35 068 [4176]	35 364 [3975]	-0.40	93.7	0.69	0.07
Total cerebral ventricles and choroid plexus volumes (mm³)	**13 313 [6433]**	**10 416 [3996]**	**2.75**	**128**	**6.8×10^{-3}**	**0.51**

Bold indicates the value with statistical significance. The $P < 0.042$ ($q = 0.25$ for 6 repeating t-tests) was determined as a statistical significance level. Abbreviation; ASD, Autism spectrum disorder; eTIV, estimated total intracranial volume; GM, gray matter; non-ASD, nonautistic controls; SD, standard deviation; WM, white matter.
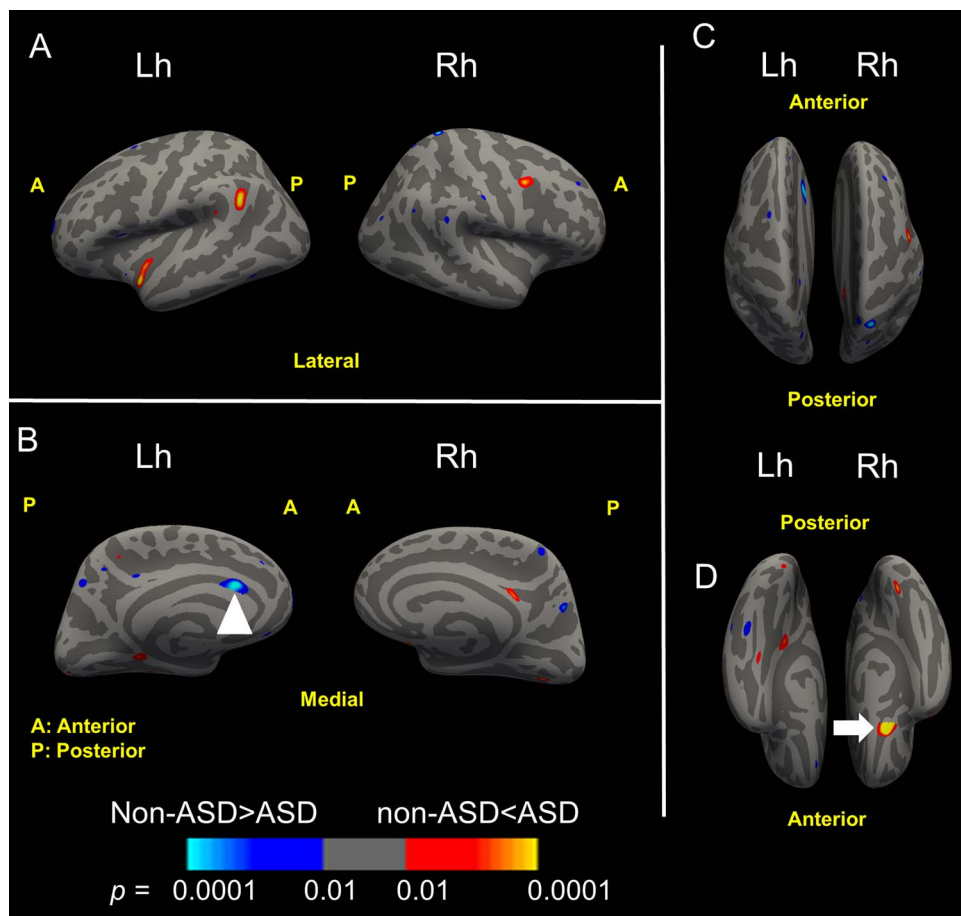

Figure 2. Surface-based vertex-wise t-statistical maps on inflated surface maps (dark gray = sulci; light gray = gyri) of thicker and thinner cortex in participants with ASD ($N = 85$) versus nonautistic controls (non-ASD, $N = 45$) in lateral (A), medial (B), dorsal (C), and ventral (D) views. Regions depicted in red–yellow and blue indicate areas with thicker and thinner cortices in ASD compared with non-ASD participants, respectively. Decreased cortical thickness in a part of the left caudal anterior cingulate cortex (B, white arrowhead) and increased cortical thickness in the right medial orbitofrontal cortex (D, white arrow) had low P-values ($P < 0.0001$). Abbreviation, Lt, left hemisphere; Rh, right hemisphere.

ventricles volume, and the rate of the NAc volume to the cerebral ventricles volume, respectively.

Discussion

We evaluated 85 structural T1-weighted MR images obtained from infants and toddlers later diagnosed with ASD. The 230

regionally distributed measurements (cortical and subcortical volumes, surface area, and cortical thickness) from the "aseg" and "aparc" annotations showed the smaller NAc and the larger cerebral ventricles, independent of covariates (age, gender, and prematurity) in the ASD compared to the non-ASD participants. The vertex-wise t-statistical map showed a thinner cortex of the left caudal ACC and a thicker cortex of the right mOF in ASD. The

Table 2 Selected cortical and subcortical measurements with statistically significant differences between ASD and non-ASD participants

Anatomical measurements ("aparc" and "aseg")	ASD (85 images) Mean [SD]	Non-ASD (45 images) Mean [SD]	t	df	P-value	Absolute Cohen's d
Forth ventricle (mm^3)	1382 [374]	1170 [285]	3.32	128	1.2×10^{-3}	0.61
Lh lateral ventricle (mm^3)	6705 [3363]	5260 [2122]	2.99	124.0	3.3×10^{-3}	0.48
Rh lateral ventricle (mm^3)	6044 [3239]	4674 [1961]	3.00	125.6	3.3×10^{-3}	0.48
Third ventricle (mm^3)	895 [294]	759 [297]	2.49	128	0.014	0.46
Rh nucleus accumbens (mm^3)	415 [107]	460 [115]	-2.19	128	0.031	0.4
Lh nucleus accumbens (mm^3)	421 [111]	465 [112]	-2.14	128	0.034	0.39

The $P < 0.058$ ($q = 0.25$ for 26 repeating t-tests) was determined as a statistical significance level. Abbreviation; ASD, Autism spectrum disorder; Lh, left hemisphere; non-ASD, nonautistic controls; Rh, right hemisphere; SD, standard deviation.

Table 3 The effects of covariates on selected brain morphologic measurements; LMM between ASD and non-ASD participants

Anatomical measurements ("aparc" and "aseg")	The presence of ASD	Gender	Age	Premature gestation	MRI scanner
Forth ventricle (mm^3)	**F = 8.80** **P = 0.004**	F = 0.35 P = 0.556	**F = 18.98** **P = 3.1×10^{-5}**	F = 5.0×10^{-4} P = 0.98	F = 1.03 P = 0.38
Lh lateral ventricle (mm^3)	**F = 6.24** **P = 0.014**	**F = 5.34** **P = 0.023**	F = 1.94 P = 0.166	**F = 4.74** **P = 0.032**	F = 0.81 P = 0.49
Third ventricle (mm^3)	**F = 5.62** **P = 0.019**	F = 2.75 P = 0.10	**F = 4.61** **P = 0.034**	F = 1.43 P = 0.234	F = 0.23 P = 0.876
Rh lateral ventricle (mm^3)	**F = 5.54** **P = 0.020**	**F = 5.08** **P = 0.026**	F = 2.23 P = 0.138	F = 4.32 P = 0.040	F = 0.63 P = 0.597
Lh nucleus accumbens (mm^3)	**F = 5.19** **P = 0.024**	F = 1.08 P = 0.301	**F = 14.03** **P = 2.9×10^{-4}**	F = 0.73 P = 0.394	F = 0.67 P = 0.570
Rh nucleus accumbens (mm^3)	**F = 4.52** **P = 0.036**	F = 0.21 P = 0.649	**F = 1.81** **P = 0.181**	F = 0.62 P = 0.431	F = 0.44 P = 0.723
Left Pallidum (mm^3)	**F = 4.40** **P = 0.038**	F = 0.67 P = 0.414	**F = 9.01** **P = 0.004**	F = 2.08 P = 0.152	**F = 3.35** **P = 0.022**
Left caudal anterior cingulate, cortical thickness (mm)	**F = 4.09** **P = 0.045**	F = 0.88 P = 0.351	F = 0.54 P = 0.465	F = 0.01 P = 0.929	**F = 3.32** **P = 0.022**

LMM analysis with confounding factors (age, gender [male 0, female 1], premature gestation) and random effect (intersubject variability). Bold indicates the value with statistically significant (P < 0.05). Abbreviation; ASD, autism spectrum disorder; Lh, left hemisphere; non-ASD, nonautistic controls; Rh, right hemisphere.

differences between ASD and non-ASD in the NAc volume and the cerebral ventricles volume were observed starting from the infantile period. These results suggest that the smaller NAc is a potential biomarker for predicting ASD, independent of other covariates.

Brain Structural MRI Studies in Infants and Toddlers with ASD

Several structural brain MRI studies in infants and toddlers with ASD have been carried out (Hazlett et al. 2005, 2011, 2012, 2017; Schumann et al. 2010; Shen et al. 2013, 2017, 2018; Wolff et al. 2015; Swanson et al. 2017; Pote et al. 2019). A prior prospective study reported overall cortical enlargement in the temporal lobe WM in 59 children with ASD at age 2 years (Hazlett et al. 2011). Another prior prospective study reported that 41 toddlers with ASD (mean age 3.6 years old) showed enlarged cerebral GM and WM in frontal, temporal, and cingulate cortices (Schumann et al. 2010). The altered morphological findings of the subcortical GM (Swanson et al. 2017) and corpus callosum (Wolff et al. 2015) have also been noted in infants with ASD. In addition, some studies in preschoolers and grade-schoolers with ASD also reported increased brain volumes in ASD (Piven et al. 1995; Courchesne et al. 2007).

Hazlett and colleagues prospectively studied structural brain MRIs from 106 infants at age 1–2 years at a high familial risk of ASD and obtained 15 examinations in ASD toddlers prior to receiving ASD diagnoses (Hazlett et al. 2017). In that study, although no group differences were observed in cortical thickness, the ASD group showed a significantly increased growth rate of the surface area from 6 to 12 months of age, predominantly in the bilateral middle occipital gyrus, right cuneus, and the right lingual gyrus (Hazlett et al. 2017).

In this study, we identified regional differences in cortical thickness between ASD and non-ASD participants. Previous studies have not focused on the cortical thickness (Hazlett et al. 2005, 2012; Schumann et al. 2010; Shen et al. 2013, 2017, 2018; Wolff et al. 2015; Swanson et al. 2017; Pote et al. 2019) except for few studies that have reported no difference in cortical thickness in ASD (Hazlett et al. 2011, 2017; Ohta et al. 2016).

A statistically significant difference in the global brain volume was not observed in our study, which is unlike considering prior studies (Schumann et al. 2010; Hazlett et al. 2011). The current study has differences from the prior studies in whether the ASD group was identified retrospectively from the patients who underwent clinical MRI or prospectively from high-risk infants, and whether non-ASD received scans for clinical purposes or as a volunteer for research.
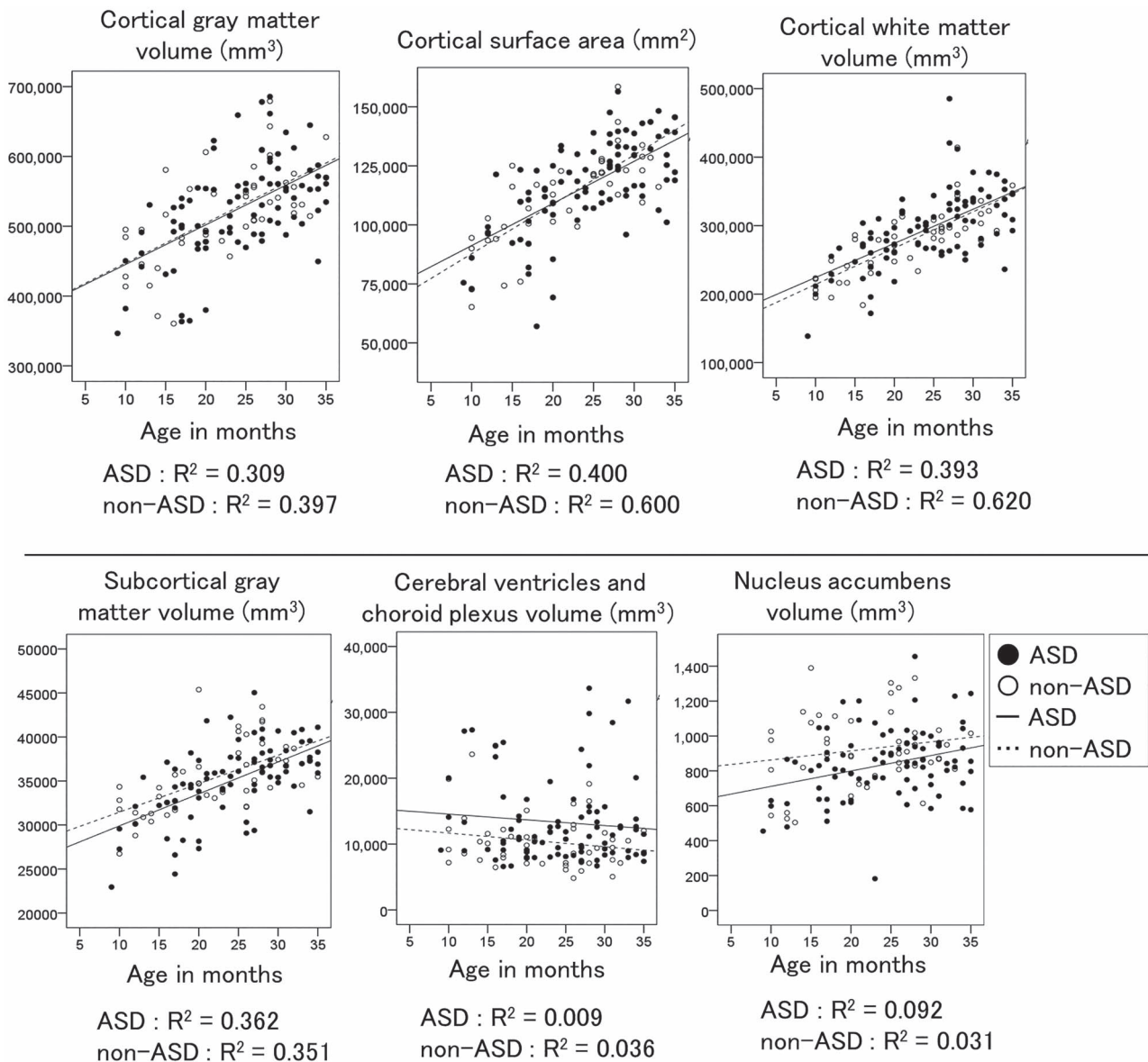
Figure 3. Scatter plots and regression lines (between age and measurements) of cortical GM, WM, subcortical GM, and cerebral ventricles and choroid plexus volume in "brainvol" annotation, cortical surface area in "aparc," and nucleus accumbens volume in "aseg" annotation in ASD (closed circle and solid-line) and non-ASD (open circle and dotted line) participants. Abbreviation; ASD, Autism spectrum disorder; GM, gray matter; non-ASD, nonautistic controls; WM, white matter.

Such difference in study designs (prospective vs. retrospective, differences in genetic risk, and exclusion of children with epilepsy and/or premature gestation) may explain the different results between the prior and current studies. Patients in most of the previous studies prospectively recruited infants at high and low genetic risks and excluded participants with premature birth (Shen et al. 2013, 2017, 2018; Wolff et al. 2015; Hazlett et al. 2017; Swanson et al. 2017; Pote et al. 2019). The participants with epilepsy were excluded in some studies (Hazlett et al. 2017; Swanson et al. 2017).

The current retrospective study excluded participants with epilepsy and/or GDD/ID and included the presence of premature gestation as a covariate. The presence of epilepsy and GDD/ID are important comorbidities that affect brain morphologic measurements. Epilepsy with an onset at young infant ages potentially includes several syndromes with a variety of severity from benign infant epilepsy to epileptic encephalopathic syndromes, which could lead to neurodevelopmental disorders such as ASD and GDD/ID. In addition, the participants with ASD and GDD/ID potentially have some undiagnosed congenital syndromes such as Rett syndrome. Therefore, in this study, we excluded participants with epilepsy and/or GDD/ID instead of including the presence of epilepsy and GDD/ID as binary variates.

NAc Volume in ASD Pathophysiology

Our results identified smaller volumes of the bilateral NAc in the ASD group compared to the non-ASD group, and the volumes of the NAc were positively associated with the volume of the
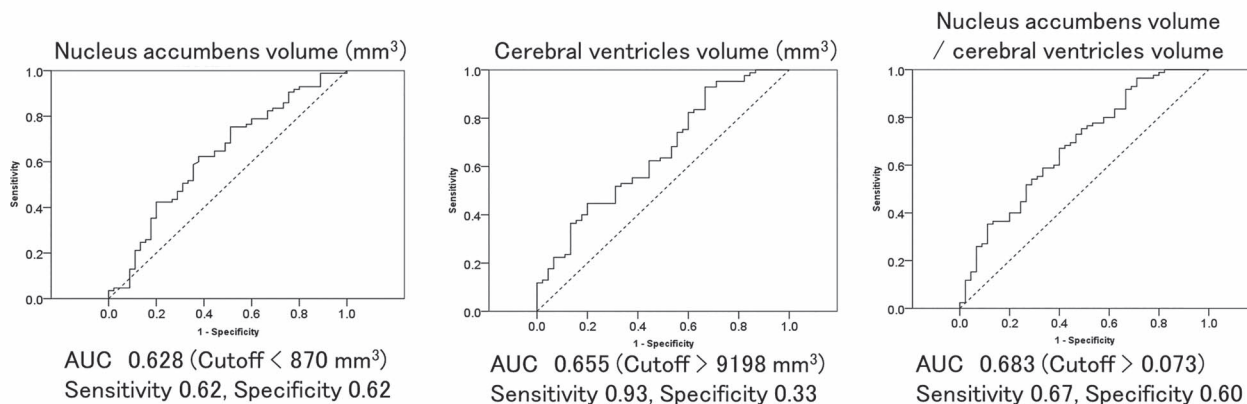
Figure 4. ROC curve for predicting the later diagnosis of ASD by the values of nucleus accumbens volume, cerebral ventricles volume, and the rate of nucleus accumbens volume to cerebral ventricles volume. Abbreviation; ASD, autism spectrum disorder; AUC, area under the curve; ROC, receiver operating characteristic.

amygdala in both groups. Previous studies of structural brain MRI in infants and toddlers with ASD have not reported volume changes in the NAc (Hazlett et al. 2005, 2011, 2012, 2017; Schumann et al. 2010; Shen et al. 2013, 2017, 2018; Wolff et al. 2015; Ohta et al. 2016; Swanson et al. 2017; Pote et al. 2019), possibly because these studies did not focus on the basal ganglia.

The NAc is a crucial component of a key neural network for maintaining flexible behavioral responses for rewards (Kehagia et al. 2010), interacting with the mOF cortex and amygdala (Jackson and Moghaddam 2001; Stuber et al. 2012; Holloway et al. 2018). Dopamine regulates behaviors associated with action selection in the striatum, reward in the NAc, emotional processing in the amygdala, and executive functioning in the mOF cortex. Such a dynamic interaction between the mOF cortex, amygdala, and the NAc may be fundamental to the regulation of goal-directed behavior by affective and cognitive processes (Jackson and Moghaddam 2001). Abnormal coordination between these regions has been suggested to underlie behavioral control deficits in neuropsychiatric disorders, as well as ASD (Stuber et al. 2012; Mannella 2013).

The neuropeptide oxytocin treatment has been reported to improve social performance in ASD patients (Yamasue et al. 2020; Watanabe et al. 2015; Gordon et al. 2016; Kruppa et al. 2019). Interestingly, the enhancement of serotonin release from the paraventricular nucleus to the NAc via binding of oxytocin receptor activation on the NAc has been widely accepted as the therapeutic mechanism of oxytocin for social performance in ASD (Dölen et al. 2013; Walsh et al. 2018). Taken together, the volume reduction of the NAc in the ASD group in our study suggests its relation to the ASD pathophysiology.

The Cerebral Ventricles in ASD Pathophysiology

In terms of the cerebral ventricles in ASD, group differences from controls in extra-axial fluid volumes were either very mild (Shen et al. 2013, 2017, 2018) or not observed in some previous infant studies (Hazlett et al. 2012; Pote et al. 2019). A review article reported that many studies rarely found ventricular volume differences in early development, but rather in adolescence and adulthood (Ismail et al. 2016). The extra-axial fluid is not in the same location as the cortical ventricle fluid is; however, our findings of large cortical ventricles in ASD are consistent with

the findings observed by Shen and colleagues (Shen et al. 2013, 2017, 2018).

Although the association between the cerebral fluid and the occurrence of ASD still remains unclear, interestingly, CSF abnormalities and ASD-hydrocephalus comorbidity have been identified from a population-based cohort study (Munch et al. 2021). In our study, using the modified version of FreeSurfer for infantile cases may have helped to detect the large cortical ventricles in early brain development.

The Right Medial Orbitofrontal Cortex in ASD Pathophysiology

Our results demonstrated the increased thickness of the right mOF in the ASD group. The pathogenic significance of the increased cortical thickness in ASD has been generally understood to be associated with synaptic pruning deficits in ASD (Geschwind and Levitt 2007; Tang et al. 2014; Khundrakpam et al. 2017). Synaptic pruning is the process that excess synapses decrease in response to neural activity and is recognized as a process to optimize network structures more economically and functionally (Navlakha et al. 2015). The process begins at perinatal stages and continues through adolescence (Khundrakpam et al. 2017). Although regional differences of synaptic pruning in typical development are not fully understood, it is possible that the thicker right insular cortex in ASD in our study may be associated with a regional deficit of synaptic pruning in ASD. This result could implicate the role of neurogenic regions responsible for brain growth and hodology, such as the subventricular zone of the lateral ventricle (Sanai et al. 2011; Corley et al. 2019) in ASD. Our results indicate that additional studies of cell activity and migratory potential in such regions warrant further attention.

The Left Caudal Anterior Cingulate Cortex in ASD Pathophysiology

We found, in the ASD group, decreased cortical thickness of the left caudal part of the anterior cingulate cortex (ACC), which is involved in the frontal executive functions, parietal sensorimotor systems, and the limbic intentional or emotional process (Holroyd and Coles 2002; Taylor et al. 2007; Zhou et al. 2016). Zhou and colleagues reported decreased functional connectivity

between the left caudal ACC and the cortical regions related with the sensorimotor networks in the ASD group using resting-state functional MRI (Zhou et al. 2016).

On the other hand, there is no unified view on the ACC and ASD pathophysiology in structural MRI studies in the literature so far. One study reported decreased cortical thickness of the right caudal ACC was identified in adults with ASD (Laidi et al. 2019), while other researchers identified increased cortical thickness of the left caudal ACC in toddlers with ASD (Jiao et al. 2010).

Advantages and Limitations in this Study

We performed a large-scale study for identifying early MRI-based biomarkers of ASD in infants and toddlers. In clinical settings at BCH, structural T1-weighted brain MRIs were scanned with the same model of MRI machines throughout the study period. Additionally, we used Infant FreeSurfer (Fischl 2012; de Macedo et al. 2015; Zöllei et al. 2020), which is optimized for infantile participants of 0–2 YO, instead of the original version of FreeSurfer. The original FreeSurfer is recommended not to use for participants under 6 YO of age, and the rate of failure increases for participants under 8 months of age, at which point myelination contrast patterns have inverted to match the general pattern exhibited through the rest of life. Infant FreeSurfer successfully extracted measurements from clinical MRI examinations for almost all participants aged 0–3 YO in this study. The images of ASD and non-ASD control groups used in this study were selected from images with a successful run on the FreeSurfer recon-all command in our previous study on ASD (Levman et al. 2018a) and non-ASD participants (Levman et al. 2017). That may be the reason why recon-all analyses of Infant FreeSurfer were successfully completed in almost all images of ASD and non-ASD participants in this study.

A limitation of this study is a lack of gold standard diagnoses for autism (ADI-R and ADOS evaluations were available in a small part of ASD participants) due to the retrospective nature of this study, which made it difficult to account for all variables tracked and controlled, but it is hoped that this work will identify anatomic and physiological effects of interest that will be thoroughly validated in carefully controlled future prospective studies.

Another limitation is that there are fewer non-ASD participants in our study than ASD participants. Because of the nature of the clinical neuroimaging at BCH, the number of available MRI images for non-ASD participants was lower than for ASD patients. Additionally, the male–female rate of ASD is generally considered to be 4:1 (Jokiranta et al. 2014). When selecting the non-ASD group, we also focused on age- and gender-matching from patients scanned by the same suit of MRI magnets and the uniformity of scan conditions, which further reduced the number of included non-ASD scans. The low rate of non-ASD to ASD participants in the group matching process potentially decreased statistical power in this study.

We also could not entirely exclude a possible presence of measurement bias by a variety of scan sequences and selection bias (healthcare access bias) with a higher rate of co-occurring clinical conditions in our sample. Comparison of our rates with those reported in a prior population-based study (Jokiranta et al. 2014) found premature birth (<37 weeks of gestation) in children with ASD were 25.6% versus 9.4%. Because our study was conducted at a single medical facility that treats more complex cases, ASD patients in our study may have had more severe conditions than the general population.

Conclusion

Statistically significant smaller bilateral accumbens nuclei and larger cerebral ventricles were identified in infants and toddlers with prospective ASD patients compared with controls, independent of age, gender, or gestational age at birth. This result suggests that there are MRI-based biomarkers in prospective ASD patients before they receive the diagnosis and that the volume of the nucleus accumbens and cerebral ventricles can be key MRI-based early biomarkers to predict the emergence of ASD.

Supplementary Material

Supplementary material can be found at *Cerebral Cortex* online.

Data Availability

The datasets generated during the current study are available from the corresponding author on reasonable request.

Author Contributions

Funding

Notes

Ethics Declarations

All procedures performed in this study were in accordance with the ethical standards of the institutional and/or national research committee and with the 1964 Helsinki declaration and its later amendments or comparable ethical standards. Ethics approval was obtained from the Boston Children's Hospital's Institutional Review Board; informed consent was waived due to the lack of risk to the patients.

References

Baio J, Wiggins L, Christensen DL, Maenner MJ, Daniels J, Warren Z, Kurzius-Spencer M, Zahorodny W, Robinson Rosenberg C,

White T, et al. 2018. Prevalence of autism spectrum disorder among children aged 8 years - autism and developmental disabilities monitoring network, 11 sites, United States, 2014. *MMWR Surveill Summ*. 67(6):1–23.

Benger M, Kinali M, Mazarakis ND. 2018. Autism spectrum disorder: prospects for treatment using gene therapy. *Mol Autism*. 9:39.

Benjamini Y, Drai D, Elmer G, Kafkafi N, Golani I. 2001. Controlling the false discovery rate in behavior genetics research. *Behav Brain Res*. 125:279–284.

Bernier R, Golzio C, Xiong B, Stessman HA, Coe BP, Penn O, Witherspoon K, Gerdts J, Baker C, Vulto-van Silfhout AT, et al. 2014. Disruptive CHD8 mutations define a subtype of autism early in development. *Cell*. 158:263–276.

Collins DL, Neelin P, Peters TM, Evans AC. 1994. Automatic 3D intersubject registration of MR volumetric data in standardized Talairach space. *J Comput Assist Tomogr*. 18:192–205.

Corley MJ, Vargas-Maya N, Pang APS, Lum-Jones A, Li D, Khadka V, Sultana R, Blanchard DC, Maunakea AK. 2019. Epigenetic delay in the neurodevelopmental trajectory of DNA methylation states in autism spectrum disorders. *Front Genet*. 10:907.

Courchesne E, Pierce K, Schumann CM, Redcay E, Buckwalter JA, Kennedy DP, Morgan J. 2007. Mapping early brain development in autism. *Neuron*. 56:399–413.

Dawson G, Rogers S, Munson J, Smith M, Winter J, Greenson J, Donaldson A, Varley J. 2010. Randomized, controlled trial of an intervention for toddlers with autism: the early start Denver model. *Pediatrics*. 125:e17–e23.

de Macedo RK, Ben-Avi E, Sliva DD, Choe MS, Drottar M, Wang R, Fischl B, Grant PE, Zöllei L. 2015. A FreeSurfer-compliant consistent manual segmentation of infant brains spanning the 0-2 year age range. *Front Hum Neurosci*. 9:21.

Desikan RS, Ségonne F, Fischl B, Quinn BT, Dickerson BC, Blacker D, Buckner RL, Dale AM, Maguire RP, et al. 2006. An automated labeling system for subdividing the human cerebral cortex on MRI scans into gyral based regions of interest. *Neuroimage*. 31:968–980.

Dölen G, Darvishzadeh A, Huang KW, Malenka RC. 2013. Social reward requires coordinated activity of nucleus accumbens oxytocin and serotonin. *Nature*. 501:179–184.

Duffy FH, Als H. 2012. A stable pattern of EEG spectral coherence distinguishes children with autism from neuro-typical controls - a large case control study. *BMC Med*. 10:64.

Fidler DJ, Bailey JN, Smalley SL. 2000. Macrocephaly in autism and other pervasive developmental disorders. *Dev Med Child Neurol*. 42:737–740.

Fischl B, Salat DH, Busa E, Albert M, Dieterich M, Haselgrove C, van der Kouwe A, Killiany R, Kennedy D, Klaveness S, et al. 2002. Whole brain segmentation: automated labeling of neuroanatomical structures in the human brain. *Neuron*. 33:341–355.

Fischl B. 2012. FreeSurfer. *Neuroimage*. 62:774–781.

Geschwind DH, Levitt P. 2007. Autism spectrum disorders: developmental disconnection syndromes. *Curr Opin Neurobiol*. 17:103–111.

Gordon I, Jack A, Pretzsch CM, Vander Wyk B, Leckman JF, Feldman R, Pelphrey KA. 2016. Intranasal oxytocin enhances connectivity in the neural circuitry supporting social motivation and social perception in children with autism. *Sci Rep*. 6:35054.

Green J, Garg S. 2018. Annual research review: the state of autism intervention science: progress, target psychological and biological mechanisms and future prospects. *J Child Psychol Psychiatry*. 59:424–443.

Hazlett HC, Poe M, Gerig G, Smith RG, Provenzale J, Ross A, Gilmore J, Piven J. 2005. Magnetic resonance imaging and head circumference study of brain size in autism: birth through age 2 years. *Arch Gen Psychiatry*. 62:1366–1376.

Hazlett HC, Poe MD, Gerig G, Styner M, Chappell C, Smith RG, Vachet C, Piven J. 2011. Early brain overgrowth in autism associated with an increase in cortical surface area before age 2 years. *Arch Gen Psychiatry*. 68:467–476.

Hazlett HC, Gu H, McKinstry RC, Shaw DW, Botteron KN, Dager SR, Styner M, Vachet C, Gerig G, Paterson SJ, et al. 2012. Brain volume findings in 6-month-old infants at high familial risk for autism. *Am J Psychiatry*. 169:601–608.

Hazlett HC, Gu H, Munsell BC, Kim SH, Styner M, Wolff JJ, Elison JT, Swanson MR, Zhu H, Botteron KN, et al. 2017. Early brain development in infants at high risk for autism spectrum disorder. *Nature*. 542:348–351.

Heunis TM, Aldrich C, de Vries PJ. 2016. Recent advances in resting-state electroencephalography biomarkers for autism spectrum disorder-a review of methodological and clinical challenges. *Pediatr Neurol*. 61:28–37.

Hicks SD, Ignacio C, Gentile K, Middleton FA. 2016. Salivary miRNA profiles identify children with autism spectrum disorder, correlate with adaptive behavior, and implicate ASD candidate genes involved in neurodevelopment. *BMC Pediatr*. 16:52.

Holloway ZR, Freels TG, Comstock JF, Nolen HG, Sable HJ, Lester DB. 2018. Comparing phasic dopamine dynamics in the striatum, nucleus accumbens, amygdala, and medial prefrontal cortex. *Synapse*. 13:e22074. doi: 10.1002/syn.22074. Epub ahead of print.

Holroyd CB, Coles MGH. 2002. The neural basis of human error processing: reinforcement learning, dopamine, and the error-related negativity. *Psychol Rev*. 109(4):679–709.

Howard JS, Stanislaw H, Green G, Sparkman CR, Cohen HG. 2014. Comparison of behavior analytic and eclectic early interventions for young children with autism after three years. *Res Dev Disabil*. 35:3326–3344.

Ismail MM, Keynton RS, Mostapha MM, ElTanboly AH, Casanova MF, Gimel'farb GL, El-Baz A. 2016. Studying autism Spectrum disorder with structural and diffusion magnetic resonance imaging: a survey. *Front Hum Neurosci*. 10:211.

Jackson ME, Moghaddam B. 2001. Amygdala regulation of nucleus accumbens dopamine output is governed by the prefrontal cortex. *J Neurosci*. 21:676–681.

Jiao Y, Chen R, Ke X, Chu K, Lu Z, Herskovits EH. 2010. Predictive models of autism spectrum disorder based on brain regional cortical thickness. *Neuroimage*. 50(2):589–599.

Jokiranta E, Sourander A, Suominen A, Timonen-Soivio L, Brown AS, Sillanpää M. 2014. Epilepsy among children and adolescents with autism spectrum disorders: a population-based study. *J Autism Dev Disord*. 44:2547–2557.

Kato K, Mizuno S, Inaba M, Fukumura S, Kurahashi N, Maruyama K, Ieda D, Ohashi K, Hori I, Negishi Y, et al. 2018. Distinctive facies, macrocephaly, and developmental delay are signs of a PTEN mutation in childhood. *Brain Dev*. 40:678–684.

Kehagia AA, Murray GK, Robbins TW. 2010. Learning and cognitive flexibility: frontostriatal function and monoaminergic modulation. *Curr Opin Neurobiol*. 20:199–204.

Khundrakpam BS, Lewis JD, Kostopoulos P, Carbonell F, Evans AC. 2017. Cortical thickness abnormalities in autism spectrum disorders through late childhood, adolescence, and

adulthood: a large-scale MRI study. *Cereb Cortex*. 27:1721–1731.

Kim YS, Fombonne E, Koh YJ, Kim SJ, Cheon KA, Leventhal BL. 2014. A comparison of DSM-IV pervasive developmental disorder and DSM-5 autism spectrum disorder prevalence in an epidemiologic sample. *J Am Acad Child Adolesc Psychiatry*. 53:500–508.

Kruppa JA, Gossen A, Oberwelland Weiß E, Kohls G, Großheinrich N, Cholemkery H, Freitag CM, Karges W, Wölfle E, Sinzig J, et al. 2019. Neural modulation of social reinforcement learning by intranasal oxytocin in male adults with high-functioning autism spectrum disorder: a randomized trial. *Neuropsychopharmacology*. 44:749–756.

Laidi C, Boisgontier J, de Pierrefeu A, Duchesnay E, Hotier S, d'Albis MA, Delorme R, Bolognani F, Czech C, Bouquet C, et al. 2019. Decreased cortical thickness in the anterior cingulate cortex in adults with autism. *J Autism Dev Disord*. 49(4):1402–1409.

Levman J, MacDonald P, Lim AR, Forgeron C, Takahashi E. 2017. A pediatric structural MRI analysis of healthy brain development from newborns to young adults. *Hum Brain Mapp*. 38:5931–5942.

Levman J, Takahashi E, Forgeron C, MacDonald P, Stewart N, Lim A, Martel A. 2018a. A sorting statistic with application in neurological magnetic resonance imaging of autism. *J Healthc Eng*. 2018:8039075.

Levman J, Vasung L, MacDonald P, Rowley S, Stewart N, Lim A, Ewenson B, Galaburda A, Takahashi E. 2018b. Regional volumetric abnormalities in pediatric autism revealed by structural magnetic resonance imaging. *Int J Dev Neurosci*. 71:34–45.

Levman J, MacDonald P, Rowley S, Stewart N, Lim A, Ewenson B, Galaburda A, Takahashi E. 2019. Structural magnetic resonance imaging demonstrates abnormal regionally-differential cortical thickness variability in autism: from newborns to adults. *Front Hum Neurosci*. 13:75.

Maenner MJ, Rice CE, Arneson CL, Cunniff C, Schieve LA, Carpenter LA, Van Naarden BK, Kirby RS, Bakian AV, Durkin MS. 2014. Potential impact of DSM-5 criteria on autism spectrum disorder prevalence estimates. *JAMA Psychiat*. 71:292–300.

Mannella F, Gurney K, Baldassarre G. 2013. The nucleus accumbens as a nexus between values and goals in goal-directed behavior: a review and a new hypothesis. *Front Behav Neurosci*. 7:135.

Monereo-Sánchez J, de Jong JJA, Drenthen GS, Beran M, Backes WH, Stehouwer CDA, Schram MT, Linden DEJ, Jansen JFA. 2021. Quality control strategies for brain MRI segmentation and parcellation: practical approaches and recommendations - insights from the Maastricht study. *Neuroimage*. 237:118174.

Munch TN, Hedley PL, Hagen CM, Bækvad-Hansen M, Bybjerg-Grauholm J, Grove J, Nordentoft M, Børglum AD, Mortensen PB, Werge TM, et al. 2021. Co-occurring hydrocephalus in autism spectrum disorder: a Danish population-based cohort study. *J Neurodev Disord*. 13(1):19.

Navlakha S, Barth AL, Bar-Joseph Z. 2015. Decreasing-rate pruning optimizes the construction of efficient and robust distributed networks. *PLoS Comput Biol*. 11:e1004347.

Ohta H, Nordahl CW, Iosif AM, Lee A, Rogers S, Amaral DG. 2016. Increased surface area, but not cortical thickness, in a subset of young boys with autism spectrum disorder. *Autism Res*. 9(2):232–248.

Pienaar R, Rannou N, Bernal J, Hahn D, Grant PE. 2015. ChRIS– A web-based neuroimaging and informatics system for collecting, organizing, processing, visualizing and sharing of medical data. *Annu Int Conf IEEE Eng Med Biol Soc*. 2015:206–209.

Piven J, Arndt S, Bailey J, Havercamp S, Andreasen NC, Palmer P. 1995. An MRI study of brain size in autism. *Am J Psychiatry*. 152:1145–1149.

Pote I, Wang S, Sethna V, Blasi A, Daly E, Kuklisova-Murgasova M, Lloyd-Fox S, Mercure E, Busuulwa P, Stoencheva V, et al. 2019. Familial risk of autism alters subcortical and cerebellar brain anatomy in infants and predicts the emergence of repetitive behaviors in early childhood. *Autism Res*. 12(4):614–627.

Reiner A, Yekutieli D, Benjamini Y. 2003. Identifying differentially expressed genes using false discovery rate controlling procedures. *Bioinformatics*. 19:368–375.

Rogers SJ, Estes A, Lord C, Munson J, Rocha M, Winter J, Greenson J, Colombi C, Dawson G, Vismara LA, et al. 2019. A multisite randomized controlled two-phase trial of the early start Denver model compared to treatment as usual. *J Am Acad Child Adolesc Psychiatry*. 58:853–865.

Sanai N, Nguyen T, Ihrie RA, Mirzadeh Z, Tsai HH, Wong M, Gupta N, Berger MS, Huang E, Garcia-Verdugo JM, et al. 2011. Corridors of migrating neurons in the human brain and their decline during infancy. *Nature*. 478:382–386.

Schumann CM, Bloss CS, Barnes CC, Wideman GM, Carper RA, Akshoomoff N, Pierce K, Hagler D, Schork N, Lord C, et al. 2010. Longitudinal magnetic resonance imaging study of cortical development through early childhood in autism. *J Neurosci*. 30:4419–4427.

Shen MD, Kim SH, McKinstry RC, Gu H, Hazlett HC, Nordahl CW, Emerson RW, Shaw D, Elison JT, Swanson MR, et al. 2017. Increased extra-axial cerebrospinal fluid in high-risk infants who later develop autism. *Biol Psychiatry*. 82(3):186–193.

Shen MD, Nordahl CW, Li DD, Lee A, Angkustsiri K, Emerson RW, Rogers SJ, Ozonoff S, Amaral DG. 2018. Extra-axial cerebrospinal fluid in high-risk and normal-risk children with autism aged 2-4 years: a case-control study. *Lancet Psychiatry*. 5(11):895–904.

Shen MD, Nordahl CW, Young GS, Wootton-Gorges SL, Lee A, Liston SE, Harrington KR, Ozonoff S, Amaral DG. 2013. Early brain enlargement and elevated extra-axial fluid in infants who develop autism spectrum disorder. *Brain*. 136(Pt 9):2825–2835.

Shiohama T, Levman J, Vasung L, Takahashi E. 2020. Brain morphological analysis in PTEN hamartoma tumor syndrome. *Am J Med Genet A*. 182:1117–1129.

Soke GN, Maenner MJ, Christensen D, Kurzius-Spencer M, Schieve LA. 2017. Brief report: estimated prevalence of a community diagnosis of autism spectrum disorder by age 4 years in children from selected areas in the United States in 2010: evaluation of birth cohort effects. *J Autism Dev Disord*. 47:1917–1922.

Srour M, Mazer B, Shevell MI. 2006. Diagnosing Sotos syndrome in the setting of global developmental delay and macrocephaly. *J Child Neurol*. 21:287–290.

Stuber GD, Britt JP, Bonci A. 2012. Optogenetic modulation of neural circuits that underlie reward seeking. *Biol Psychiatry*. 71:1061–1067.

Swanson MR, Shen MD, Wolff JJ, et al. 2017. Subcortical brain and behavior phenotypes differentiate infants with autism versus language delay. *Biol Psychiatry Cogn Neurosci Neuroimaging*. 2:664–672.

Tang G, Gudsnuk K, Kuo SH, Cotrina ML, Rosoklija G, Sosunov A, Sonders MS, Kanter E, Castagna C, Yamamoto A, et al. 2014. Loss of mTOR-dependent macroautophagy causes autistic-like synaptic pruning deficits. *Neuron*. 83:1131–1143.

Taylor SF, Stern ER, Gehring WJ. 2007. Neural systems for error monitoring: recent findings and theoretical perspectives. *Neuroscientist*. 13(2):160–172.

The American Psychiatric Association. 2013. *Diagnostic and statistical manual for mental disorders*. 5th ed.: APA DSM-5.

Vivanti G, Kasari C, Green J, Mandell D, Maye M, Hudry K. 2018. Implementing and evaluating early intervention for children with autism: where are the gaps and what should we do? *Autism Res*. 11:16–23.

Walsh JJ, Christoffel DJ, Heifets BD, Ben-Dor GA, Selimbeyoglu A, Hung LW, Deisseroth K, Malenka RC. 2018. 5-HT release in nucleus accumbens rescues social deficits in mouse autism model. *Nature*. 560:589–594.

Watanabe T, Kuroda M, Kuwabara H, Aoki Y, Iwashiro N, Tatsunobu N, Takao H, Nippashi Y, Kawakubo Y, Kunimatsu A, et al. 2015. Clinical and neural effects of six-week administration of oxytocin on core symptoms of autism. *Brain*. 138:3400–3412.

Wolff JJ, Gerig G, Lewis JD, Soda T, Styner MA, Vachet C, Botteron KN, Elison JT, Dager SR, Estes AM, et al. 2015. Altered corpus callosum morphology associated with autism over the first 2 years of life. *Brain*. 138:2046–2058.

Yamasue H, Okada T, Munesue T, Kuroda M, Fujioka T, Uno Y, Matsumoto K, Kuwabara H, Mori D, Okamoto Y, et al. 2020. Effect of intranasal oxytocin on the core social symptoms of autism spectrum disorder: a randomized clinical trial. *Mol Psychiatry*. 25:1849–1858.

Zhou Y, Shi L, Cui X, Wang S, Luo X. 2016. Functional connectivity of the caudal anterior cingulate cortex is decreased in autism. *PLoS One*. 11(3):e0151879.

Zöllei L, Iglesias JE, Ou Y, Grant PE, Fischl B. 2020. Infant FreeSurfer: an automated segmentation and surface extraction pipeline for T1-weighted neuroimaging data of infants 0-2 years. *Neuroimage*. 218:116946.

Zwaigenbaum L, Bauman ML, Choueiri R, Kasari C, Carter A, Granpeesheh D, Mailloux Z, Smith Roley S, Wagner S, Fein D, et al. 2015. Early intervention for children with autism spectrum disorder under 3 years of age: recommendations for practice and research. *Pediatrics*. 136: S60–S81.